Phase-Insensitive All-Optical Transistors Based on Second-Order Nonlinearities

Sungwon Kim, Zuo Wang, David J. Hagan, Eric W. Van Stryland,
Andrey Kobyakov, Falk Lederer, and Gaetano Assanto

***Abstract*—We demonstrate and compare two phase-insensitive all-optical transistors (AOT's) based on frequency-degenerate quadratic three-wave interactions. In particular, we demonstrate gain using KTP in a type II geometry. Both AOT's exploit the phase insensitivity inherent to three-wave parametric processes when only two fields are input, providing amplification of a small signal at the operating frequency via the interaction with a second-harmonic wave. The first scheme is based on successive up- and down-conversion (i.e., cascading) while the second relies on parametric down-conversion. We obtain gains of 5 and 160 in the two configurations, respectively, with a significant background and output coherent to the pump in the first case, no background and coherence between output and signal in the second.**

***Index Terms*—Nonlinear optics, optical amplifiers, optical materials/devices, optical parametric amplifiers, optical switches.**

I. Introduction

SINCE THE early days of nonlinear optics, researchers have been looking for all optical means to mimic the operations of electronic devices [1]. The optical Kerr effect, i.e., an intensity-dependent refractive index, has been a prime candidate for use in all-optical processing and switching together with degenerate four-wave mixing and other phenomena stemming from a cubic susceptibility [2]. More recently, the nonlinear phase shift induced by the transfer of energy between fundamental and second-harmonic waves (i.e., cascaded second-order nonlinearities) has been indicated as a viable alternative for these purposes [3], [4], offering the additional advantage of lower power requirements in technologically well-developed noncentrosymmetric materials [5], [6]. Moreover, interactions based on quadratic effects are in most cases coherent and, in specific configurations, provide the possibility for both/either phase (PM) and/or amplitude (AM) modulation [7]. Several schemes have been envisaged for achieving all-optical switching both in bulk and in guided-wave geometries [5], [6], [8], including all-optical modulation and transistor action [9]–[12]. In the latter class, the possibility of a phase-controlled transistor through second-harmonic generation (SHG) was discussed by Russell [9] and demonstrated by Hagan *et al.* [10] in a KTP crystal using the phase of a coherent second harmonic (SH) seed as the signal. Modulation contrast ratios as large as $8:1$ were reported with a SH seed having a fluence 1% of the fundamental frequency (FF) pump. While the demonstrated modulator opened up a range of interesting possibilities for coherent all-optical signal processing, it presents significant technological problems for using multiple devices since it requires that the signal be coherent with respect to the "power supply," i.e., the pump. Additionally, the necessity of a seed at the SH frequency can be undesirable. These problems prompted the investigation of transistor schemes able to amplify a signal at the operating frequency without a coherent relationship to the pump. Configurations based on type II SHG are potentially viable solutions because they rely on a three-wave parametric interaction in which only two waves are injected to the crystal [12]–[14]. Moreover, the input signal and output can be at the same frequency with amplification provided by a pump wave either at the fundamental or at the SH frequency. We will refer to the former as the "cascading transistor" (CT) and to the latter as the "parametric down-converting transistor" (PDCT).

The CT utilizes the high sensitivity of type II SHG efficiency to any imbalance between the amplitudes of the orthogonally polarized input FF waves. If one imposes a small modulation on one of the inputs while the other remains fixed, this can result in a large modulation of the conversion efficiency and hence the transmitted FF [12]. This concept has been experimentally demonstrated by Lefort and Barthelemy [15] and by Assanto *et al.* [16] in KTP crystals, and employed by Krumbugel *et al.* as an optical switch in a Kerr gate geometry [17]. Even though no phase relationship is required between the two inputs, coherence must be maintained between the small signal and one of the FF pumps in order for the device to operate as a small-signal amplifier. More recently, Wang *et al.* [18] suggested a method to impose a modulation on one of the inputs with a mutually incoherent signal through an additional coupler stage. This two-stage configuration consists of a coupler stage followed by the amplifier and benefits from an initial superposition of signal and pump through Type II SHG in the first crystal (the coupler). The resulting modulated pump is combined with the unmodulated, orthogonally polarized pump in the second SHG crystal (CT) that provides small-signal amplification. The

Manuscript received November 13, 1997; revised December 17, 1997. This work was supported in part by the National Science Foundation under Grant ECS 9320308. The work of G. Assanto and E. Van Stryland was supported by NATO under Grant CRG931142. The work of A. Kobyakov and F. Lederer was supported by a Grant from the Volkswagen Stiftung, Hannover.

S. Kim, Z. Wang, D. J. Hagan, and E. W. Van Stryland are with the Center for Research and Education in Optics and Lasers, University of Central Florida, Orlando, FL 32816-2700 USA.

A. Kobyakov and F. Lederer are with the Institute of Solid State Theory and Theoretical Optics, Friedrich-Schiller-Universität Jena, 07743 Jena, Germany.

G. Assanto is with the Department of Electronic Engineering, Terza University of Rome, 00146 Rome, Italy.

Publisher Item Identifier S 0018-9197(98)02387-2.

output of this device is an amplified signal, which is coherent with the modulated pump. This two-stage cascading transistor (TSCT) will be discussed in Section III.

The PDCT is based on down-conversion of a pump wave at twice the signal and output frequency ω. When either of the orthogonally polarized fields at ω is injected, it will trigger the energy conversion from the pump to both ω components, resulting in a substantial amplification of the signal. Since only two fields are present at the input, this scheme is also phase-insensitive and, moreover, it operates with either polarization of the input signal field. However, it requires an initial frequency conversion to obtain the SH pump. The output is then a coherently amplified form of the signal.

In this paper, we report a preliminary experimental investigation of the TSCT (Section III) and the PDCT (Section IV) schemes using KTP at the operating wavelength of 1064 nm, briefly discussing their models and underlying physics and their respective peculiar features.

II. Fundamental Equations

The standard evolution equations for slowly varying plane-wave field envelopes at frequencies ω and 2ω through a type II phase-matched quadratic susceptibility are

$$\begin{aligned}\frac{dE_1}{dz} &= i\frac{\omega}{4cn_1}\chi^{(2)}(-\omega;\,2\omega,\,-\omega)E_{2\omega}E_2^*e^{i\Delta kz}\\ \frac{dE_2}{dz} &= i\frac{\omega}{4cn_2}\chi^{(2)}(-\omega;\,2\omega,\,-\omega)E_{2\omega}E_1^*e^{i\Delta kz}\\ \frac{dE_{2\omega}}{dz} &= i\frac{\omega}{2cn_{2\omega}}\chi^{(2)}(-2\omega;\,\omega,\,\omega)E_1E_2e^{-i\Delta kz}\end{aligned}\tag{1}$$

where $\chi^{(2)}$ is the second-order susceptibility, n_i the respective linear indices, and Δk is the wavevector mismatch, $\Delta k = k(2\omega) - k_1(\omega) - k_2(\omega)$. The subscripts 1, 2 denote the two orthogonally polarized fundamental inputs and 2ω stands for the SH. In the absence of loss (i.e., applying Kleinman symmetry), $\chi^{(2)}(-\omega;\,2\omega,-\omega) = \chi^{(2)}(-2\omega;\,\omega,\,\omega)$.

For the special case of phase-matched SHG with the amplitude of the SH initially zero, exact expressions for the irradiances can be written in terms of Jacobian elliptic functions

$$\begin{aligned}I_1(z) &= I_1(0) - I_<(0)\,\mathrm{sn}^2(\Gamma_>z,\,\gamma)\\ I_2(z) &= I_2(0) - I_<(0)\,\mathrm{sn}^2(\Gamma_>z,\,\gamma)\\ I_{2\omega}(z) &= 2I_<(0)\,\mathrm{sn}^2(\Gamma_>z,\,\gamma)\end{aligned}\tag{2}$$

where sn is the Jacobian elliptic sine function, $I_>(0)$ $[I_<(0)]$ is the larger (smaller) of $I_1(0)$ and $I_2(0)$, and the modulus is given by [19], [20]

$$\gamma = \sqrt{\frac{I_<(0)}{I_>(0)}}$$

and

$$\Gamma_> = \frac{4\pi d_{\mathrm{eff}}}{\lambda}\sqrt{\frac{I_>(0)}{c\varepsilon_0 n_1 n_2 n_{2\omega}}}.$$

These general equations are used in what follows. A complete theoretical analysis of the solutions to (1) including phase evolution of any participating wave is given by Kobyakov and Lederer [21]. Equation (2) for the case of $\gamma \neq 1$ corresponds to a periodic exchange of power between the three interacting waves even in perfect phase matching. The period tends to infinity in the limit of perfectly balanced FF inputs, i.e., $I_>(0) = I_<(0)$, but becomes finite as soon as a slight input imbalance is introduced. Such large changes in the characteristic interaction length will determine, for any limited propagation distance in a realistic crystal, an abrupt variation in conversion efficiency or, equivalently, in FF throughput. This mechanism, analyzed in detail in [11] and [21], is at the basis of an imbalance-controlled all-optical transistor in type II SHG crystals.

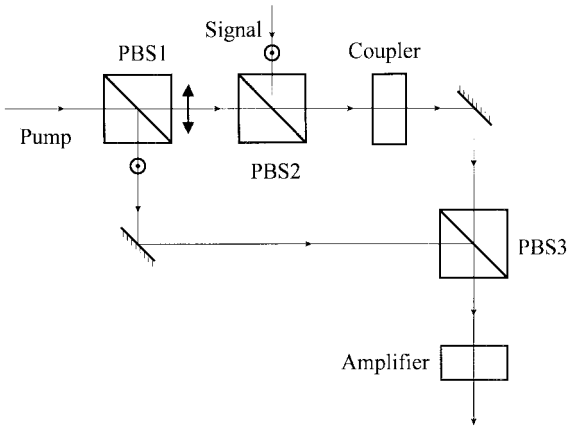

Fig. 1. Schematic of an all-optical transistor based on cascaded second-order nonlinearities. PBS: polarizing beam splitter.

III. The Two-Stage Cascading Transistor (TSCT)

The experimental schematic for a phase-insensitive AOT based on cascaded second-order nonlinearities is shown in Fig. 1. A Gaussian beam from a 1.064-μm Q-switched and mode-locked Nd : YAG laser producing single, switched-out, 30-ps FWHM pulses at a repetition rate of 10 Hz is used as the source. In this experiment, two type II KTP crystals are used as the frequency-doubling nonlinear crystals. At the polarizing beam splitter (PBS1), the pump beam is split into two approximately equal but orthogonally polarized pump beams. One of the pump beams (Pump1, I_{pump1}) and an orthogonally polarized weak signal (Signal, I_{signal}) are combined via a second polarizing beam splitter (PBS2) and interact in the first type II KTP crystal, the *Coupler*. Here the Signal is a split-off portion of the pump beam (not shown); however, it is important to note that this signal need not be coherent with respect to Pump 1 to weakly modulate it through SHG as was verified experimentally (see below). Using an additional beam splitter (PBS3), this modulated pump beam is recombined collinearly with the other pump beam (Pump2, I_{pump2}) and input to the second type II KTP crystal, the *Amplifier*. Here the weak modulation is strongly amplified through the second-order nonlinearity.

At the Coupler crystal, the transmitted intensity of Pump1 is

$$I_{\mathrm{pump1}}(L_1) = I_{\mathrm{pump1}}(0) - I_{\mathrm{signal}}(0)\,\mathrm{sn}^2(\Gamma_1 L_1,\,\gamma_1)\tag{3}$$

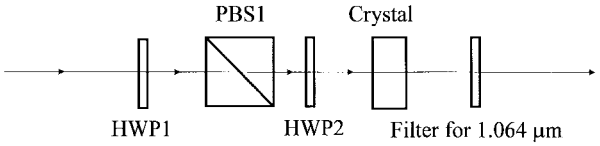

Fig. 2. Measurement apparatus for characterizing the Coupler and Amplifier crystals. HWP's are half-wave plates.

where

$$\Gamma_1 = \frac{4\pi d_{\text{eff}}}{\lambda}\sqrt{\frac{I_{\text{pump1}}(0)}{c\varepsilon_0 n_1 n_2 n_{2\omega}}}$$

$$\gamma_1 = \sqrt{\frac{I_{\text{signal}}(0)}{I_{\text{pump1}}(0)}}. \tag{4}$$

The period of the square of the Jacobian elliptic sine function is $2K(\gamma_1)$, where $K(\gamma_1)$ is the complete Jacobian elliptic integral of the first kind. The squared sine function is maximum at $\Gamma_1 L_1 = (2q+1)K(\gamma_1)$ with q an integer. For a weak signal $I_{\text{signal}}(0) \ll I_{\text{pump1}}(0)$, terms of order γ_1^3 and higher can be neglected, and we can write [19]

$$K(\gamma_1) \approx \frac{\pi}{2}\left(1+\frac{\gamma_1^2}{4}\right).$$

Thus, in order to obtain the most efficient coupling, the intensity of Pump1 must satisfy

$$I_{\text{pump1}}(0) \approx (2q+1)^2\,\frac{c\varepsilon_0 n_1 n_2 n_{2\omega}\lambda^2}{64 d_{\text{eff}}^2 L_1^2}\left(1+\frac{\gamma_1^2}{2}\right). \tag{5}$$

If we consider temporal pulses, the irradiances of the Pumps must be changed in order to maximize the coupling. Similarly if the Gaussian spatial profiles are averaged, the optimum conditions need to be adjusted accordingly. Averaging in time or space or both reduces the coupling, and in order to maintain its value the irradiance required becomes higher than that for the plane-wave CW case. Before testing the complete AOT of Fig. 1, we evaluated the performance of the two basic components, the Coupler and the Amplifier separately.

Each crystal was mounted in a three-axis goniometric stage for phase-match adjustment. We first measured the transmittance of the fundamental beam after the KTP Coupler crystal using the experimental configuration shown in Fig. 2. The ratio of the two orthogonally polarized input beams, Pump 1 and Signal, was controlled by a half-wave plate (HWP2 in Fig. 2). Fixing the ratio of the Pump and Signal, we measured the fundamental output energy modulation while changing the input energy by rotating a half-wave plate (HWP1). The experimental results for two KTP crystal lengths are shown in Fig. 3 along with numerical predictions. We chose the 2-mm crystal as the Coupler since it exhibited the best modulation for the irradiance needed at the Amplifier. A Signal that is 5% of $I_{\text{pump1}} = 1.56$ GW/cm^2 at the Coupler can give 3% energy depletion on Pump 1. As we describe below, the necessary irradiance is determined by the amplifier crystal in combination with the amplitude fluctuations (i.e., noise) of our laser system.

In order to find an optimum operating point that maximized the useable gain in the Amplifier [as defined by our signal-to-noise ratio (SNR)], we investigate the Amplifier alone by changing the ratio of the two pump beams. This is accomplished by rotating HWP2 in Fig. 2. The result is shown in Fig. 4. Here the Amplifier crystal was a 5-mm-long KTP crystal, and the total pump irradiance was 2.0 GW/cm^2 (i.e., sum of the irradiances of both pump beams). We chose the operating point marked in Fig. 4 where the slope, and hence gain, was maximum. The transmittance curve near this operating point has a constant slope giving linear gain, and this point allows the largest dynamic range for linear amplification.

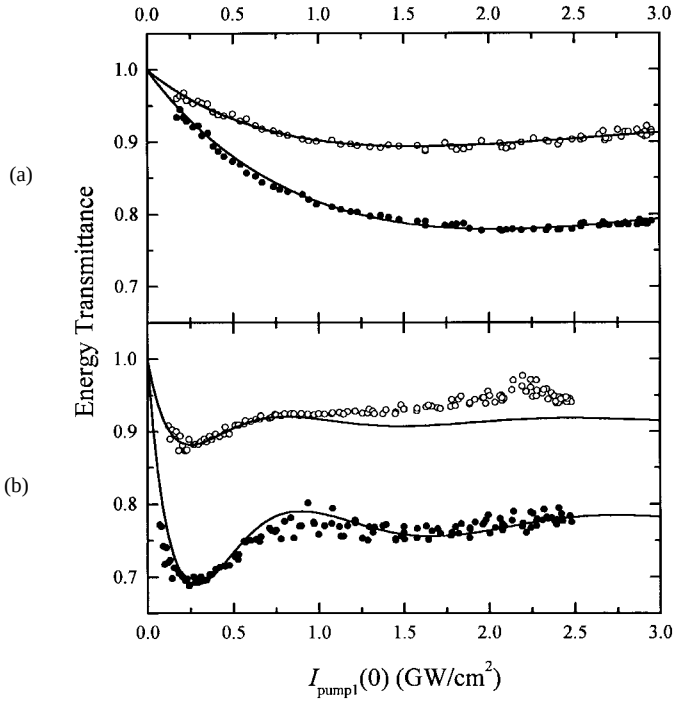

Fig. 3. Transmittance of the Coupler as a function of Pump1 for different ratios of Signal to Pump1 in (a) a 2-mm and (b) a 5-mm KTP crystal. The open circles are data for a Signal to Pump ratio of 0.15 in energy for the 2-mm crystal and 0.17 for the 5-mm crystal while the closed circles are data for a ratio of 0.30 for the 2-mm crystal and 0.42 for the 5-mm crystal. The solid lines are the results of numerical modeling. The input irradiance I_{pump1} was fixed at 1.6 GW/cm^2.

In the TSCT transistor experiments, we attempted to mimic this operating point, however, with I_{pump1} optimized for the Coupler, we obtain $I_{\text{pump1}} = 0.82$ GW/cm^2 and $I_{\text{pump2}} = 0.92$ GW/cm^2 at the Amplifier. This reduction in irradiance was due to losses at optical components in the path as well as free-space propagation between the Coupler and Amplifier. At this operating point, we applied the Signal. The pulse energy transmittances as well as the on-axis peak-fluence transmittance of Pump 1 and Pump 2 were measured after the amplifier. The fluence was measured by placing a small aperture in the beam after the amplifier crystal at a short-enough distance that free-space propagation effects could be neglected. This evaluation gives a measure of how well this type of device would work in a two-dimensional waveguide geometry, where spatial averaging does not take place due to propagation in a confined waveguide mode. In our results, the quoted fluence gain was scaled to account for the slight beam expansion ($\cong$20% increase in spot size) due to diffraction between input and output.

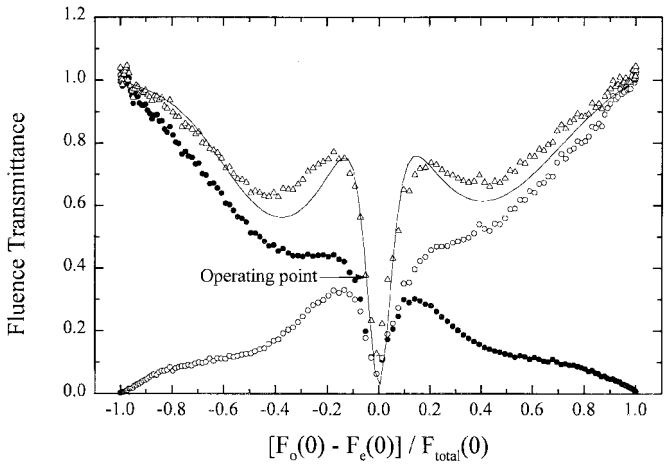

Fig. 4. Transmittance of on-axis fluence for a 5-mm KTP Amplifier crystal while changing the ratio of an ordinary beam to an extraordinary beam. $F_o(0)$ and $F_e(0)$ denote the input fluence of the ordinary and extraordinary Pump beams, respectively. The transmittances are: solid circles, F_o; open circles. F_e; triangles, $F_o = F_e$. The total pump irradiance ($I_{\mathrm{pump}1} + I_{\mathrm{pump}2}$) is 2.0 GW/cm^2 and the total fluence is 0.062 J/cm^2.

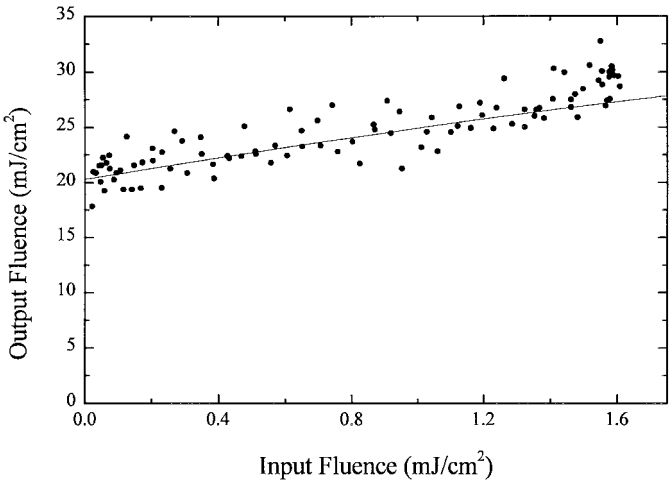

Fig. 5. Output on-axis fluence versus input on-axis fluence for the AOT of Fig. 1. The solid circles are data and the solid line is the result of the numerical model.

Fig. 5 shows the fluence transmittance of the cascaded AOT, the input being the sum of Pump 1 and Pump 2. The graph shows a gain of 5.2 with a large constant background, while numerical simulations give a gain of 5.3. The measured energy gain is $\cong$2. We checked to see that the output is independent of the phase of the input signal with respect to the pump by varying the optical path length of the Signal prior to the transistor. No change in output was observed for pathlength changes of many wavelengths. As mentioned above, the large background could be eliminated using an analyzer at the output provided the two light paths in Fig. 1 were held interferometrically stable. Then the polarizer would select just the polarization containing the Signal, despite the lack of coherence between Signal and Pump. We did not implement this approach due to experimental limitations. Alternatively, for digital applications where linearity and dynamic range are less important than in analog devices, one could operate near the zero imbalance point (which corresponds to the separatrix [22]), greatly reducing the background as well. For the operating point in the experiments reported here, the contrast ratio of total signal to background is approximately 1.3 at the maximum input as seen in Fig. 5. Moving the operating point closer to zero imbalance could increase this parameter by as much as one order of magnitude with the same gain.

A. Noise Characteristics

The measured SNR was low in large part due to the significant background. In these experiments the signal and pump were derived form the same source so that the noise was additive. Eliminating the background, which constituted about 80% of the output, would reduce the noise by about 80%, thus greatly increasing the SNR and allowing significantly higher irradiances and an increased gain. We estimate the noise properties in what follows.

The analytical study of noise in the framework of the exact formulas (2) is fairly involved because noise affects both the argument and the modulus of the elliptic sn-function. Hence, it is reasonable to approximate this function near the operating point (Fig. 4) by elementary functions. If the modulus γ of the elliptic function is close to unity, which implies a small imbalance between the two FF components (a situation encountered in the experiment), we may write

$$\mathrm{sn}^2(x, \gamma) \approx \tanh^2(x - T) \tag{6}$$

where T is the period of the squared sn-function. Under the same assumption for the period we have

$$T = 2K(\gamma) \approx 2\tau - (1-\tau)(1-\gamma^2)/2 \tag{7}$$

where $K(\gamma)$ is the complete elliptic integral of the first kind and $\tau = \ln(4/\sqrt{1-\gamma^2})$. If both FF components are of the order of 1 GW/cm^2 and their relative difference is about 10% or less, the second term in (7) can be neglected. This approximation amounts to an error of only a few percent compared to (2). Substituting (6) and (7) into (2), we get an approximate expression for the total FF irradiance at the output

$$I_{\mathrm{out}}^{\mathrm{FF}} \approx I_<^0 + I_>^0 - 2I_<^0\left(\frac{U_- - qU_+}{U_- + qU_+}\right)^2 \tag{8}$$

where the weaker $I_<(0)$ and the stronger $I_>(0)$ orthogonally polarized FF components are denoted by $I_<^0$ and $I_>^0$, respectively, and

$$U_\pm = 1 \pm \tanh\left(\rho\sqrt{I_>^0}\right),\ q = \left(\frac{1-\gamma^2}{16}\right)^2$$
$$\rho = \frac{4\pi d_{\mathrm{eff}} L}{\lambda\sqrt{c\varepsilon_0 n_1 n_2 n_{2\omega}}} \tag{9}$$

where L is the crystal length. Equations (8) and (9) can be exploited to study the noise properties of the TSCT. Assuming that the FF pump is subject to noise and the PBS used is ideal, i.e., the noise is split like the signal, we can calculate the moments of the randomly changed output FF irradiance. Notice that the most important noise characteristic is the width (or dispersion) of the output distribution of the FF irradiance

which corresponds to the second moment. Defining the noise parameter δ as the deviation of the total input FF irradiance $I_>^0 + I_<^0$ from the mean value, the first-order term in the expansion of (8) is written as

$$w_{\mathrm{TSCT}} \approx 1 - \frac{2\overline{I}_<}{\overline{I}_< + \overline{I}_>}\left(\frac{U_- - qU_+}{U_- + qU_+}\right)^2 + 8q\rho\,\frac{\overline{I}_<\sqrt{\overline{I}_>}(U_- - qU_+)}{\overline{I}_< + \overline{I}_>(U_- + qU_+)^3}\,\mathrm{sech}^2\left(\rho\sqrt{\overline{I}_>}\right) \tag{10}$$

where ρ, q, and $U_\pm$ are given by (9) with initial values $I_{>,<}(z=0)$ are replaced by their mean values $\overline{I}_>$, $\overline{I}_<$ (equal to the initial values with the noise averaged). Thus, the width of the output distribution is

$$W_{\mathrm{TSCT}} = \sqrt{\overline{[I_{\mathrm{out}}^{\mathrm{FF}} - \overline{I}_{\mathrm{out}}^{\mathrm{FF}}]^2}} = |w_{\mathrm{TSCT}}|\sqrt{\overline{\delta^2}} \tag{11}$$

where the overstrike here and in what follows indicates mean value. The width of the input noise distribution $\sqrt{\overline{\delta^2}}$ characterizes the laser source. For example, for a flat input distribution with 5% deviation from the mean value, this width is 0.029. The dependence of (10) is graphed in Fig. 6(a) as a function of $\overline{I}_>/\overline{I}_<$ for constant $\overline{I}_< = 0.82$ GW/cm^2 assuming elimination of the large background ($\lambda = 1.06\,\mu$m, $n_{1,2,2\omega} = 1.76$, $d_{\mathrm{eff}} =$ 3.1 pm/V, and $L = 5$ mm). The corresponding gain is plotted in Fig. 6(b). From the plot it is apparent that the maximum gain nearly coincides with the maximum of the noise transmittance and that noise is suppressed for some ratios $\overline{I}_>/\overline{I}_<$. However, for a more rigorous treatment, higher order terms should be taken into account in deriving (10). When the background is not eliminated, noise from this undesired component of the pump beam is also present on the output, greatly decreasing the SNR. Finally, we must also note that these calculations performed in the CW plane-wave case do not include the temporal (and spatial) averaging inherent in the experimental measurements. In general, such averages lower effects by the order of $\sqrt{2}$ per dimension.

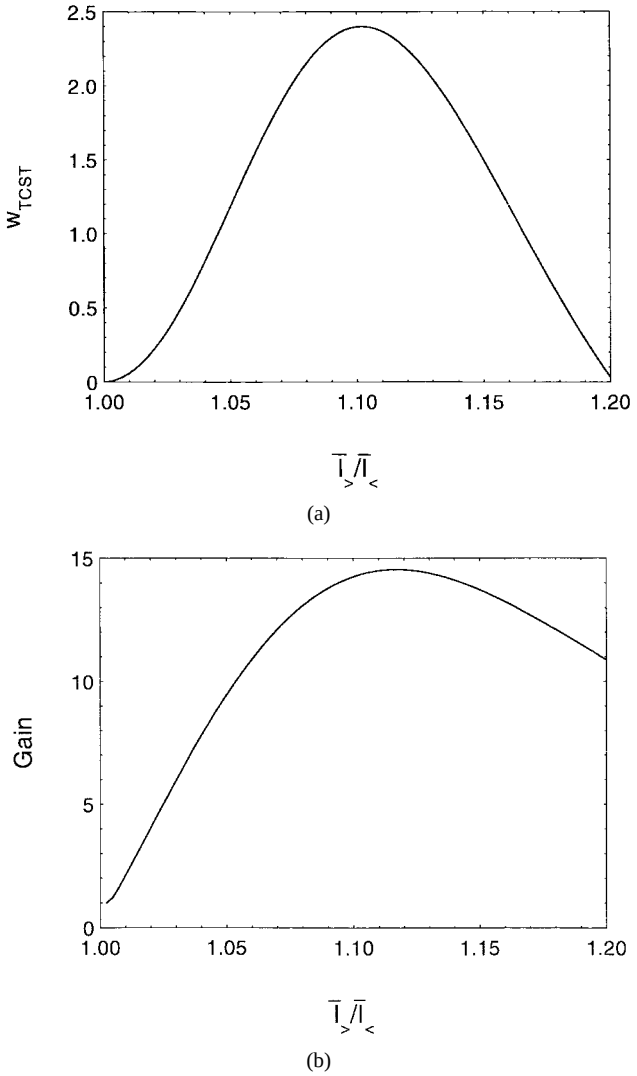

Fig. 6. (a) w_{TSCT} of (10) as a function of the ratio of averaged FF components $\overline{I}_>/\overline{I}_<$ for $\overline{I}_< = 0.82$ GW/cm^2 and (b) the corresponding gain.

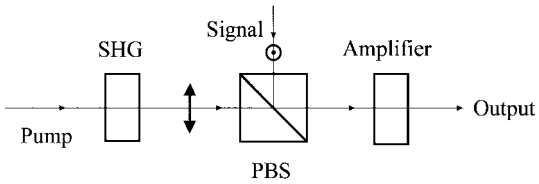

Fig. 7. Schematic of an all-optical transistor based on parametric down-conversion.

IV. Parametric Down-Converting Transistor (PDCT)

Here we discuss the well-known phenomena of parametric amplification used in order to accomplish a similar function to the cascaded AOT, i.e., the amplification of an arbitrary phase fundamental Signal [23]. In the present case, however, a strong SH wave is the power supply (Pump). In the experiments, the Coupler of the previous section is replaced by a crystal (either type I or II) to produce a large pump at the second harmonic. Fig. 7 shows the experimental schematic for this AOT. As in Section III, the second crystal must be cut and oriented for type II SHG and acts as the Amplifier. The Signal is input directly to the second crystal and is polarized perpendicular to the SH pump. While the output in the TSCT is coherent to the Pump, in the PDCT the amplified FF output is coherent with the Signal. This is a fundamental difference and could have implications on the use of either device.

If the Signal is very weak with respect to the SH wave, the fundamental outputs can be expressed in the undepleted pump approximation as [19], [21]

$$I_1(L) = I_1(0)\,\cosh^2(\Gamma L)$$
$$I_2(L) = I_1(0)\,\sinh^2(\Gamma L) \tag{12}$$

where

$$\Gamma = \frac{4\pi d_{\mathrm{eff}}}{\lambda}\sqrt{\frac{I_{2\omega}(0)}{2c\varepsilon_0 n_1 n_2 n_{2\omega}}}.$$

Under this assumption we can write the signal gain as

$$\mathrm{Gain} \cong \cosh^2(\Gamma L) + \sinh^2(\Gamma L) = \cosh(2\Gamma L). \tag{13}$$

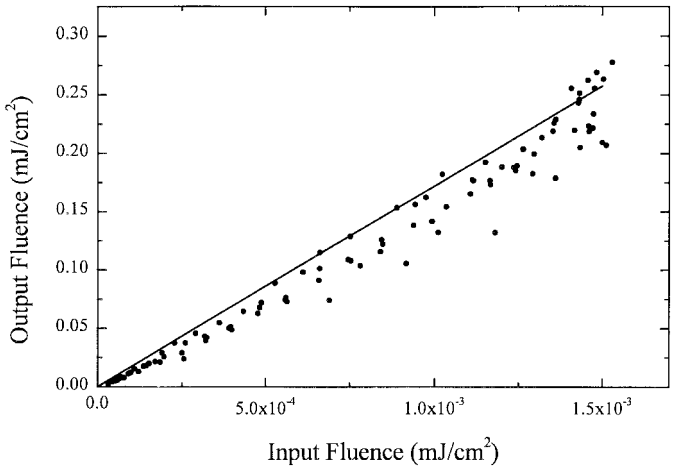

Fig. 8. Output on-axis fluence versus input on-axis fluence of the AOT of Fig. 7. The solid circles are data and the solid line is the result of the numerical model.

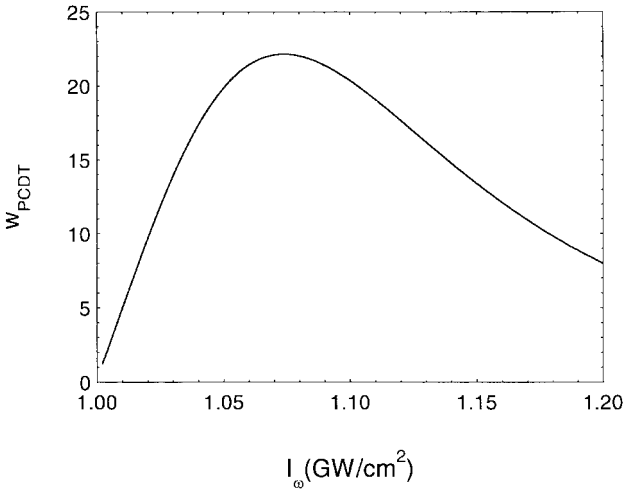

Fig. 9. The dependence of the noise transmittance w_{PDCT} of (17) on the irradiance of the small FF signal I_ω^0. The averaged SH pump irradiance is $\overline{I}_{2\omega} = 1.0$ GW/cm^2.

However, this estimation is quite crude and valid only when the down-conversion of the FF wave does not exceed an efficiency of ≅2%. Therefore, using the exact formulas, instead of (12) and (13) we write the total irradiance of the amplified signal at the output of the amplifier as [19], [22]

$$I_{\mathrm{FF}}(L) = I_\omega^0\left[1 + 2\beta^2 \mathrm{sd}^2\left|\rho\sqrt{(I_\omega^0 + I_{2\omega}^0/2)}, \beta\right|\right] \tag{14}$$

where $\mathrm{sd}(x) = \mathrm{sn}(x)/\mathrm{dn}(x)$ is the Jacobi elliptic sd-function with modulus $\beta = \sqrt{I_{2\omega}^0/(2I_\omega^0 + I_{2\omega}^0)}$. Here $I_\omega^0 = I_>(z = 0)$ while $I_<(z = 0) = 0$ for the FF irradiances at the input, and $I_{2\omega}^0 = I_{2\omega}(0)$, with ρ determined by (9). This is valid for a CW plane-wave FF Signal, and SH Pump, but, for a pulsed source and/or a Gaussian beam in space, the fluence/energy of the fundamental output is inevitably reduced. The experimental result for the on-axis fluence gain is shown in Fig. 8 after appropriate scaling to account for the small beam diffraction with propagation. The fluence gain is ≅160 using 1.0 GW/cm^2 SH pump and a maximum Signal of 45 kW/cm^2. The numerical models give a fluence gain of 170 and, as expected, a reduced energy gain of 37.

A. Noise Properties of the PDCT

An approximate expression written in terms of elementary functions for the output FF intensity required to study the noise influence is

$$I_{\mathrm{out}}^{\mathrm{FF}} \approx I_\omega^0 + I_{2\omega}^0\left[1 - \left(\frac{V_- - rV_+}{V_- + rV_+}\right)^2\right] \tag{15}$$

where

$$V_\pm = 1 \pm \tanh\left(\rho\sqrt{I_\omega^0 + I_{2\omega}^0/2}\right),\ r = I_\omega^0/\lfloor 8(2I_\omega^0 + I_{2\omega}^0)\rfloor \tag{16}$$

with ρ given in (9). Equations (15) and (16) provide good accuracy even for the limit of strong pump depletion.

As in the previous section, assuming a "noisy" pump, the transmittance of input noise related to the width of the output FF irradiance can be easily calculated

$$w_{\mathrm{PDCT}} \approx 1 - \left(\frac{V_- - rV_+}{V_- + rV_+}\right)^2 + 2\overline{I}_{2\omega} r\,\frac{\rho\sqrt{I_\omega^0 + \overline{I}_{2\omega}/2} - 1}{I_\omega^0 + \overline{I}_{2\omega}/2} \cdot \frac{V_- - rV_+}{(V_- + rV_+)^3}\,\mathrm{sech}^2\left(\rho\sqrt{I_\omega^0 + \overline{I}_{2\omega}/2}\right). \tag{17}$$

Here $\overline{I}_{2\omega}$ is the mean value of $I_{2\omega}^0$ and this value also appears in $V_\pm$ and r is given by (16). The corresponding width characteristics are presented in Fig. 9 as a function of the FF signal irradiance for a constant mean value of the pump $\overline{I}_{2\omega} =$ 1 GW/cm^2 using the same material parameters as for Fig. 6. As can be inferred from Fig. 9, the influence of the pump noise in the PDCT increases with the input FF signal corresponding to an increased conversion efficiency. For a particular value of I_ω^0, the width of the output distribution reaches a maximum and then decreases. Such behavior is similar to that plotted in Fig. 6 for the TSCT which, however, exhibits an output distribution varying over a wider interval revealing a range where noise suppression may be possible. For shorter pulse durations, a temporal averaging in the presence of walk-off should be included in (10) and (17), as discussed in [23].

V. Conclusion

We have demonstrated two distinct implementations of an all-optical transistor based on second-order nonlinearities in simple amplifier geometries. Neither implementation requires mutual coherence between the signal and the pump. The first, based on second-order cascading, imposes a modulation on the power supply which is subsequently amplified resulting in an output which is coherent with the pump but not with the input signal. The substantial constant background superimposed to the output could be eliminated by proper polarization filtering or by operating in the nonlinear region of the characteristic (see Fig. 4). For the analog case (i.e., linear performance) which we experimentally demonstrate in this paper, we expect this would also allow considerably higher gains associated to higher pump irradiances. The second AOT, based on

parametric amplification through down-conversion, directly and coherently amplifies the signal without a background. The experiments performed show superior performance of the parametric device, with larger gain and a substantially higher SNR. However, for cases where an output is needed that is an imposed modulation on a strong light beam (pump) the cascaded geometry may be desirable.

Either scheme could be the specific solution to a particular application. For example, both transistors may be used as wavelength converters while acting as switches or amplifiers. In the cascading transistor the modulation could be induced on one of the pumps through a sum frequency generation process with an arbitrary frequency signal in the coupler. This would allow for simultaneous amplification and wavelength conversion to a different communication channel in WDM-based systems. In demultiplexing, any frequency signal could be returned to the desired operating wavelength of a strong pump. A similar channel switching can be accomplished with the parametric down conversion device by using the perpendicularly polarized "idler" as the output with the pump shifted from its second harmonic, i.e., with the output consisting of an amplified signal at the input signal frequency ω_s plus a second one at a shifted frequency $\omega_s + \Delta$, with $\omega_s + (\omega_s + \Delta)_i = \omega_p = 2\omega_s + \Delta$ [24].

REFERENCES

[1] H. M. Gibbs and G. Khitrova, *Nonlinear Photonics.* Berlin, Germany: Springer-Verlag, Springer Series in Electronics and Photonics, vol. 30, 1990.

[2] G. P. Agrawal, *Nonlinear Fiber Optics.* San Diego, CA: Academic, 1989.

[3] R. DeSalvo, D. J. Hagan, M. Sheik-Bahae, G. Stegeman, E. W. Van Stryland, and H. Vanherzeele, "Self-focusing and self-defocusing by cascaded second-order effects in KTP," *Opt. Lett.,* vol. 17, pp. 28–30, 1992.

[4] G. I. Stegeman, M. Sheik-Bahae, E. W. Van Stryland, and G. Assanto, "Large nonlinear phase shifts in second-order nonlinear optical processes," *Opt. Lett.,* vol. 18, pp. 13–15, 1993.

[5] G. Assanto, G. I. Stegeman, M. Sheik-Bahae, and E. W. Van Stryland, "All optical switching devices based on large nonlinear phase shifts from second harmonic generation," *Appl. Phys. Lett.,* vol. 62, pp. 1323–1325, 1993.

[6] R. Schiek, "Nonlinear refraction caused by cascaded second-order nonlinearity in optical waveguide structures," *J. Opt. Soc. Amer. B,* vol. 10, pp. 1848–1855, 1993.

[7] G. Assanto, G. I. Stegeman, M. Sheik-Bahae, and E. Van Stryland, "Coherent interactions for all-optical signal processing via quadratic nonlinearities," *IEEE J. Quantum Electron.,* vol. 31, p. 673, 1995.

[8] C. N. Ironside, J. S. Aitchison, and J. M. Arnold, "An all optical switch employing the cascaded second-order nonlinear effect," *IEEE J. Quantum Electron.,* vol. 29, p. 2650, 1993.

[9] P. St. J. Russell, "All-optical high gain transistor using second-order nonlinearities," *Electron. Lett.,* vol. 29, pp. 1228–1229, 1993.

[10] D. J. Hagan, M. Sheik-Bahae, Z. Wang, G. Stegeman, E. W. Van Stryland, and G. Assanto, "Phase controlled transistor action by cascading of second-order nonlinearities," *Opt. Lett.,* vol. 19, p. 1305, 1994.

[11] G. Assanto, I. Torelli, and S. Trillo, "All-optical phase controlled amplitude modulator," *Electron. Lett.,* vol. 30, p. 733, 1994.

[12] G. Assanto and I. Torelli, "Cascading effects in Type II second-harmonic generation: Applications to all-optical processing," *Opt. Commun.,* vol. 119, p. 143, 1995.

[13] D. C. Hutchings, J. S. Aitchison, and C. N. Ironside, " All-optical switching based on nondegenerate phase shifts from a cascaded second-order nonlinearity," *Opt. Lett.,* vol. 18, p. 10, 1993.

[14] D. N. Klyshko and B. F. Polkovnikov, "Phase modulation and self-modulation of light in three-photon processes," *Sov. J. Quantum Electron.,* vol. 3, pp. 324–326, 1974.

[15] L. Lefort and A. Barthelemy, *Opt. Lett.,* vol. 20, pp. 1749–1751, 1995; see also L. Lefort and A. Barthelemy, "All-optical transistor action by polarization rotation during type-II phase-matched second harmonic generation," *Electron. Lett.,* vol. 31, pp. 910–911, 1995.

[16] G. Assanto, Z. Wang, D. J. Hagan, and E. W. Van Stryland, "All-optical modulation via nonlinear cascading in type II second-harmonic generation," *Appl. Phys. Lett.,* vol. 67, pp. 2120–2122, 1995.

[17] M. A. Krumbugel, J. Sweetser, D. Fittinghoff, K. DeLong, and R. Trebino, "Ultrafast optical switching by use of fully phase-matched cascaded second-order nonlinearities in a polarization-gate geometry," *Opt. Lett.,* vol. 22, pp. 245–247, 1997.

[18] Z. Wang, D. J. Hagan, E. W. Van Stryland, and G. Assanto, "Phase-insensitive, single wavelength, all-optical transistor based on second-order nonlinearities," *Electron. Lett.,* vol. 32, p. 1135, 1996.

[19] P. F. Byrd and M. D. Friedman, *Handbook of Elliptic Integrals for Engineers and Scientist,* 2nd ed. New York: Springer-Verlag, 1971.

[20] J. A. Armstrong, N. Bloembergen, J. Ducuing, and P. S. Pershan, "Interaction between light waves in a nonlinear dielectric," *Phys. Rev.,* vol. 127, pp. 1918–1939, 1962.

[21] A. Kobyakov and F. Lederer, "Cascading of quadratic nonlinearities—An analytical study," *Phys. Rev. A,* vol. 54, pp. 3455–3472 1996.

[22] A. Kobyakov, U. Peschel, R. Muschall, G. Assanto, V. P. Torchigin, and F. Lederer, "Analytical approach to all-optical modulation by cascading," *Opt. Lett.,* vol. 20, pp. 1686–1688, 1995.

[23] A. Kobyakov, E. Schmidt, and F. Lederer, "The effect of group velocity mismatch on amplitude and phase modulation of picosecond pulses in quadratically nonlinear media," *J. Opt. Soc. Amer. B,* vol. 14, pp. 3242–3252, 1997.

[24] S. J. B. Yoo, "Wavelength conversion techniques for WDM network applications," *J. Lightwave Technol.,* vol. 14, pp. 955–966, 1996.

Sungwon Kim, photograph and biography not available at the time of publication.

Zuo Wang, photograph and biography not available at the time of publication.

David J. Hagan, photograph and biography not available at the time of publication.

Eric W. Van Stryland, photograph and biography not available at the time of publication.

Andrey Kobyakov, photograph and biography not available at the time of publication.

Falk Lederer, photograph and biography not available at the time of publication.

Gaetano Assanto, photograph and biography not available at the time of publication.